

1 **INVESTIGATING THE EFFECT OF ASPHALT PAVEMENT TEXTURE ON**  
 2 **TIRE/ROAD NOISE: A FINITE ELEMENT METHOD-BOUNDARY**  
 3 **ELEMENT METHOD (FEM-BEM) BASED APPROACH**  
 4  
 5  
 6  
 7  
 8  
 9

10 Lei ZHANG

11 PhD Candidate, Department of Civil & Environmental Engineering

12 National University of Singapore

13 Block E1A, 1 Engineering Drive 2, #07-03, Singapore 117576

14 Phone: +65 6601-2651, Fax: +65 6516-1635

15 E-mail: a0068326@nus.edu.sg

17 Ghim Ping ONG (Corresponding Author)

18 Assistant Professor, Department of Civil & Environmental Engineering

19 National University of Singapore

20 Block E1A, 1 Engineering Drive 2, #07-03, Singapore 117576

21 Phone: +65 6516-2279, Fax: +65 6516-1635

22 E-mail: ceeongr@nus.edu.sg

24 Tien Fang FWA

25 Professor, Department of Civil & Environmental Engineering

26 National University of Singapore

27 Block E1A, 1 Engineering Drive 2, #07-03, Singapore 117576

28 Phone: +65 6516-2276, Fax: +65 6516-1635

29 E-mail: ceefwatf@nus.edu.sg

33 Total Number of Words (Reference excluded)

34 Number of words in text: = 5208 words equivalent

35 Number of tables: 2 (2\*250) = 500 words equivalent

36 Number of figures: 8 (8\*250) = 2000 words equivalent

37 -----

38 Total number of words = 7708 words equivalent

42 Submitted for presentation and publication in the  
 43 94th Transportation Research Board Annual Meeting

47 July 2014

1  
2 **INVESTIGATING THE EFFECT OF ASPHALT PAVEMENT TEXTURE ON**  
3 **TIRE/ROAD NOISE: A FINITE ELEMENT METHOD-BOUNDARY**  
4 **ELEMENT METHOD (FEM-BEM) BASED APPROACH**

5  
6 By:

7 L. Zhang, G. P. Ong and T. F. Fwa  
8

9 **ABSTRACT**

10  
11 Traffic noise has become a major health concern in the modern environment. Noise  
12 generated from tire-pavement interaction is a major source of traffic noise at high  
13 speeds. Besides improvement in tire technologies in reducing tire-pavement noise,  
14 improvement in pavement surface properties also plays an important role reducing  
15 tire-road noise. However, there is a lack of mechanistic simulation model that can  
16 properly model the effect of pavement texture on tire-road noise. This paper therefore  
17 investigates the effect of pavement texture on tire/road noise using a numerical  
18 simulation model combining finite element method (FEM) and boundary element  
19 method (BEM). Four sub-steps are integrated in the model, namely rotation analysis,  
20 modal analysis, vibration analysis and BEM acoustic simulation. The close-proximity  
21 (CPX) test using a smooth tire is simulated using this model. Noise levels on twelve  
22 test sections paved with five surface types (ISO standard surface, thin layered asphalt,  
23 stone mastic asphalt, dense asphalt concrete and surface dressing) are next  
24 investigated using the developed model to study the effect of pavement type, texture  
25 depth and aggregate size on CPX noise level. It was found that pavement type  
26 significantly affects noise emission and tire/road noise increases with the increase in  
27 pavement texture depth and nominal maximum aggregate size.  
28  
29

## 1 INTRODUCTION

2  
3 Road traffic noise is one of the major contributors to environmental pollution in urban  
4 regions. It annoys people, disturbs sleep patterns, causes stresses and diseases, and  
5 disrupts daily activities. den Boer and Schrotten (1) reported that 44% of the people  
6 staying in Europe were regularly exposed to road traffic noise of over 55 dB - a level  
7 which may cause negative health effects - with a societal costs of over €40 billion per  
8 year (which is about 0.4% of total annual gross domestic product of the European  
9 Union). Over the years, there has been a significant reduction in vehicle powertrain  
10 noise and as a result of that, the main noise source from a vehicle traveling at high  
11 speed is from the interaction between tire and pavement surface. Tire/road noise  
12 dominates traffic noise at speeds above 40 km/h for passenger cars and 60 km/h for  
13 trucks which is well within the range of normal highway operating speeds (2).

14 Tire/road noise is a complex combination of many noise generation  
15 mechanisms. These mechanisms can be broadly divided into two categories, namely  
16 tire vibration phenomena and aerodynamic effects. Tire vibrations are induced by  
17 pavement texture, tire rotation and frictional force. Aerodynamic effects include air  
18 turbulence, air pumping, groove resonance and air resonant radiation (3). Amongst  
19 these noise generation mechanisms, tire-road noise generated from tire wall vibration  
20 is perhaps the dominant noise generation mechanism under most traveling conditions  
21 (4).

22 Past experimental studies on tire vibration noise are often limited in number  
23 and scale. This is due to the difficulties in isolating the structure-borne noise from the  
24 overall noise recorded by the microphones or other noise-measuring instruments.  
25 Koizumi et al. (5) measured the tire vibration noise generated by a rolling smooth tire  
26 using a scanning laser Doppler vibrometer and found that the measured sound  
27 intensity was related to tire vibration behavior. Kindt et al. (6) performed experiments  
28 to study how driving speed, cleat dimension, inflation pressure, tire temperature and  
29 preload can affect structure-borne noise. It was found that there is a significant  
30 difference between the natural frequencies of rolling and non-rolling tires and that tire  
31 cavity resonances did not have a significant contribution to structure-borne noise.  
32 Cesbron et al. (7) found from their experiments that pavement macrotexture generates  
33 contact forces with frequencies at around 800 Hz and close-proximity noise levels  
34 with frequency ranging between 500 and 1000 Hz.

35 Since the early 2000s, emphasis were placed in the development of  
36 analytical/numerical tire vibration noise models. Kim (8) developed a theoretical  
37 model where the tire was represented by a circular ring and tire motion was described  
38 by a set of thin shell equations. Sound power was related to normalized frequency and  
39 structural loss factor. The basic sound radiation mechanism was shown to be a  
40 damped progressive wave field on the tire. Fujikawa et al. (9) examined the influence  
41 of road roughness on tire vibration noise and found that pavement asperity height,  
42 asperity unevenness, asperity radius and asperity spacing can affect tire vibration  
43 noise. O'Boy and Dowling (10) developed an analytical model where the tire belt was  
44 modelled as a multilayer viscoelastic cylinder and the pavement was described by an  
45 equivalent simple bending plate model. Far-field noise was predicted in their works  
46 through the use of transfer functions.

47 Finite element method (FEM) and boundary element method (BEM) are  
48 widely in tire/road noise modeling. One such model was established by Brinkmeier et

1 al. (11) where the tire simulation was decomposed into three components: a nonlinear  
2 stationary rolling case, an eigenvalue analysis on deformed tire and a noise radiation  
3 prediction module. Arbitrary Lagrangian Eulerian (ALE) algorithm was adopted to  
4 simplify the kinematic description of the rolling tire and a combined finite/infinite  
5 element technique was used to compute the acoustic response from structure vibration.  
6 Another rolling tire noise model was developed by Kropp et al. (12) using the  
7 waveguide finite element method (WFEM) to calculate mode amplitude and replicate  
8 tire vibration during rolling. Sound pressure level around the tire was computed using  
9 boundary element method. This model was used to identify the contribution of  
10 individual mode to the radiated sound power. It was found that low-order modes are  
11 responsible for the sound radiation at the 1000 Hz frequency range.

12 Although various methods have been explored in the literature in developing  
13 tire vibration noise simulation models (8-13), they are focused on reducing tire/road  
14 noise through the optimization of tire design and are less interested in reducing  
15 tire/road noise from the pavement perspective. This paper therefore attempts to  
16 develop a tire/road noise simulation model that can be used to study the influence of  
17 pavement texture on tire/road noise emission. A numerical model combining both  
18 finite element and boundary element methods is developed. The model is calibrated  
19 and validated and then applied to predict the noise level for a tire rolling on various  
20 pavement surfaces. The effect of pavement surface texture, texture depth and  
21 aggregate size on noise emission from the rolling tire is then studied.

## 22 23 **DEVELOPMENT OF TIRE/ROAD NOISE SIMULATION MODEL**

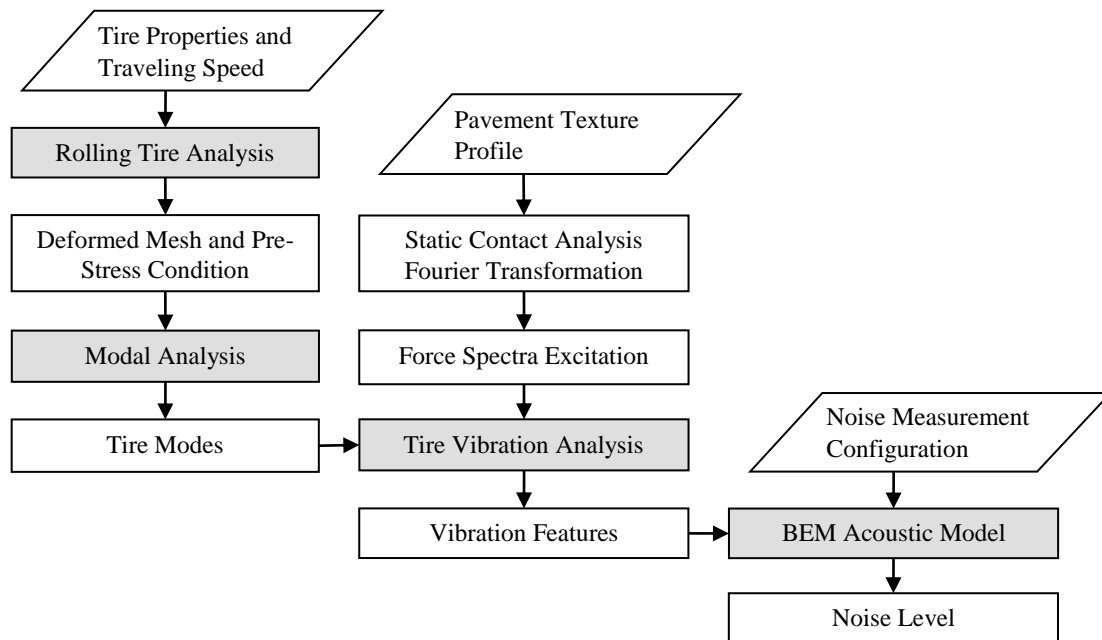
24  
25 In this paper, a tire/road noise simulation scheme similar to those used in  
26 references (11) and (12) is used to develop a numerical simulation model to predict  
27 the rolling tire noise induced by pavement texture. The overall framework is shown in  
28 Figure 1. There are four major steps, namely rolling tire analysis, modal analysis, tire  
29 vibration analysis and BEM acoustic simulation. With input parameters such as tire  
30 properties and vehicle operating conditions defined, the deformations and stresses  
31 developed on tire walls can be determined. Natural frequencies and mode shapes of  
32 the rolling tire can be determined from modal analysis and tire vibration  
33 characteristics are predicted through mode superposition using the excitation from  
34 pavement texture as an input variable. Tire vibrations are then used in the BEM  
35 acoustic simulation model to estimate the sound field around a rolling tire.

### 36 37 **Rolling Tire Analysis**

38  
39 FEM has been used for rolling tire simulations in the literature (14-16). Both steady  
40 state rolling analysis and explicit dynamic rolling simulation have been developed to  
41 analyze tire performance and pavement reaction. The explicit dynamic approach is  
42 adopted in this paper. A relative motion frame of reference is used to facilitate the  
43 model configuration (Figure 2). In this frame of reference, wheel is rolling without  
44 horizontal translation, while the pavement moves towards the standing tire at a  
45 specified vehicle traveling speed. Only vertical translation is allowed on a cylindrical  
46 rigid axle. A pneumatic tire model is assembled onto the axle with a revolution joint  
47 connection pair defined at the interface where only rotation is allowed at this point.  
48 The tire is modeled by three components, namely tire tread, tire sidewalls and tire rim.

1 The tire interacts with the pavement surface through a frictional contact (which is  
 2 defined at the tire-pavement interface). The pavement surface is assumed rigid and a  
 3 sufficient pavement length is modeled to ensure that the tire has complete at least  
 4 three full revolutions on the pavement surface.

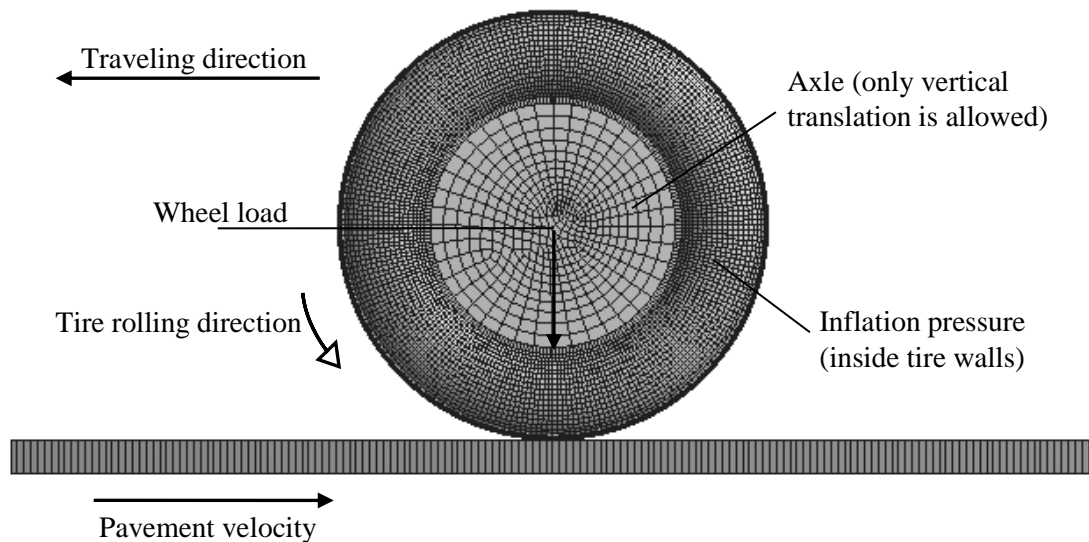
5



6

7 **FIGURE 1 Framework of tire/road noise prediction model.**

8



9

10 **FIGURE 2 Relative motion frame of reference for a rolling tire.**

11

12 The radial tire is a complex composite structure constructed by a number of  
 13 rubber components and reinforcements and as such, some simplification is necessary  
 14 to make the numerical simulation efficient. The laminated composite theory (17) is  
 15 used to convert multiple-layer tire component into a single layer, which is then  
 16 modeled using shell elements in FE model. The successful use of shell elements in tire  
 17 modeling has been validated by numerous past research works (18-20). The frictional

1 contact between tire tread and pavement surface is modeled using Coulomb's Law and  
 2 the augmented Lagrangian algorithm is used to solve this nonlinear contact problem.

3 The rolling tire analysis is sub-divided into three load steps. The first step  
 4 involves the application of a uniform pressure onto the inner surfaces of tire walls to  
 5 simulate tire inflation. Vertical wheel load is then gradually added onto the axle in the  
 6 second step, pushing the tire against the pavement surface. Tire rotation is introduced  
 7 in the third load step by adding a translational velocity on the pavement and a  
 8 corresponding angular velocity on the tire. The deformed mesh and stresses developed  
 9 on tire walls obtained from this analysis are then extracted and used as inputs to the  
 10 tire modal analysis.

### 11 **Tire Modal Analysis**

12 Natural frequencies and mode shapes are essential tire vibration properties considered  
 13 in the development of tire-pavement noise simulation model. They are related to the  
 14 geometry and composition of the tire itself. In the tire modal analysis, the frequency  
 15 response functions of the nodes on tire walls are determined so that the tire responses  
 16 to a certain frequency excitation can be derived. The modal analysis attempts to solve  
 17 the eigen-problem defined in Equation (1).

$$20 [K]\{\phi\} = \lambda[M]\{\phi\} \quad (1)$$

21 where  $[K]$  is the structure stiffness matrix,  $[M]$  is the structure mass matrix,  $\{\phi\}$  is the  
 22 eigenvector, and  $\lambda$  is the eigenvalue. For a pre-stressed modal analysis, the stress  
 23 stiffness matrix  $[S]$  is included in the  $[K]$  matrix. By definition, the eigenvalues are the  
 24 roots of characteristic polynomial i.e.  $\det([K] - \lambda[M]) = 0$ , while eigenvectors are the  
 25 nontrivial solutions of Equation (1) corresponding to each  $\lambda$ . The integrated scheme  
 26 for large-scale gyroscopic eigenvalue extraction proposed by Brinkmeier and  
 27 Nackenhorst (21) is adopted in this paper to generate natural frequencies and mode  
 28 shapes for rolling tires.

29 Modal analysis is performed on the deformed tire geometry obtained from the  
 30 rolling tire analysis and the mode shapes at frequencies up to 3000 Hz are extracted  
 31 for the tire vibration analysis. Modes at higher frequencies are neglected as low-order  
 32 modes were found in the literature to be responsible for tire/road noise generation (12).

### 34 **Tire Vibration Analysis**

35 When a tire is rolling on a road surface, its dynamic characteristics create fluctuating  
 36 forces that excite tire wall vibrations. The mode superposition method (22) is widely  
 37 used in the literature to study tire vibration behavior due to its efficiency and ease of  
 38 implementation. This method is used in this paper to predict tire vibration resulting  
 39 from pavement texture excitation. The equation of motion is expressed as:

$$41 [M]\{\ddot{u}\} + [C]\{\dot{u}\} + [K]\{u\} = \{F\} \quad (2)$$

42 where:  $[C]$  is damping matrix and  $\{F\}$  is load vector. A set of modal coordinates  $y_i$  is  
 43 defined so that the displacement vector can be related to all the mode shapes:

$$44 \{u\} = \sum_{i=1}^n \{\phi_i\} y_i \quad (3)$$

1 where  $\{\phi_i\}$  is the mode shape of mode  $i$  and  $n$  is the number of modes to be used.  
 2 Substituting Equation (3) into Equation (2) yield the following formula:

$$3 \quad \ddot{y}_j + 2\xi_j\omega_j\dot{y}_j + \omega_j^2y_j = \{\phi_j\}^T \{F\} \quad (4)$$

4 Equation (4) represents  $n$  uncoupled equations with  $n$  unknowns  $y_i$  ( $i$  from 1 to  $n$ ) For  
 5 the knowne load vector  $\{F\}$ , the modal coordinates  $y_i$ , and the displacement vector  $\{u\}$   
 6 can be computed using Equation (3).

7 It is noted that the load vector  $\{F\}$  in Equation (4) is a summation of the loads  
 8 derived from all critical modes and the nodal excitation forces due to pavement  
 9 surface texture. The former is obtained from the tire modal analysis while the latter is  
 10 computed from a static FE tire model which uses the measured texture spectrum as an  
 11 applied displacement load onto the tire-pavement contact patch (23). The reaction  
 12 forces on tire tread are then computed and the external nodal force spectrum is applied  
 13 on all the tire nodes in the tire-pavement contact patch. Together with the loads  
 14 computed from the modal analysis and the load vector  $\{F\}$  in Equation (4), the tire  
 15 wall displacements, vibration velocities and accelerations in frequency domain can be  
 16 obtained as the output.

17

## 18 **Boundary Element Model for Acoustic Simulation**

19

20 Boundary element method (BEM) is next used to simulate sound propagation in the  
 21 air using tire vibrations as the source of noise generation. The integral form of  
 22 Helmholtz equation on boundary relates the boundary pressure and normal velocity by  
 23 a matrix equation:

$$24 \quad [A]\{p\} = [B]\{v_n\} \quad (5)$$

25 where  $[A]$  and  $[B]$  are coefficient matrices. The velocity boundary conditions are  
 26 applied to Equation (5) and the pressures at boundaries are solved. The acoustic field  
 27 pressures are next solved from the integration of boundary solutions of acoustic  
 28 pressure and normal velocity:

$$29 \quad p(r) = \{C\}^T \{p\} + \{D\}^T \{v_n\} \quad (6)$$

30 where  $\{C\}$  and  $\{D\}$  are coefficient vectors derived from the integral-form Helmholtz  
 31 equation on boundary.

32 The deformed tire geometry generated from the rolling tire analysis is  
 33 imported into the BEM model. Vibration velocities on tire surfaces obtained from tire  
 34 vibration analysis are then mapped onto the acoustic mesh. The dense-graded asphalt  
 35 pavement is modeled as an acoustically hard surface. The mass density of air is set to  
 36 be  $1.225 \text{ kg/m}^3$  and the sound velocity is  $340 \text{ m/s}$ . The acoustic pressure in air field  
 37 around a rolling tire can then be computed together with other acoustic characteristics.  
 38 The sound pressure level at CPX microphone positions is computed from the pressure  
 39 obtained from the BEM simulation. It is a logarithmic measure of the effective sound  
 40 pressure relative to a reference value:

$$41 \quad L_p = 10 \cdot \log \left( \frac{p}{p_0} \right) \quad (7)$$

42 where  $L_p$  is the sound pressure level,  $p$  is the acoustic pressure at a specific position,  
 43 and  $p_0 = 20 \text{ } \mu\text{Pa}$  is the standard reference sound pressure.

44

## 1 MODEL CALIBRATION AND VALIDATION

2  
3 It is difficult to segregate tire vibration noise from the overall tire-pavement noise in  
4 most practical noise measurements. Although tire vibration is the main component,  
5 some other noise generation mechanisms such as air pumping and groove resonance  
6 may also exist during the tire rolling process. As these mechanisms are not captured  
7 by the developed model, a careful calibration has to be carried out before the model  
8 can be used for noise prediction. The calibration process is realized by an  
9 optimization process scaling the tire mode shapes. The mode shape vector  $\{\phi_i\}$  for  
10 each mode  $i$  is unique in shape, but does not have unique amplitude. It can be  
11 arbitrarily scaled with the constant relationship between each component. A scaling  
12 constant  $a_i$  is defined for mode  $i$  so that the modal mass  $m_i$  is expressed as

$$13 \quad m_i = \frac{1}{a_i \omega_i} \quad (8)$$

14 where  $\omega_i$  is the natural frequency of mode  $i$ . Scaling constant  $a_i$  is taken as variable in  
15 the optimization process and objective function is to minimize the difference between  
16 simulated noise level and measured result in the interested frequency range of 1/3  
17 octave spectrum:

$$18 \quad \min z = \sum |L_s - L_m| \quad (9)$$

19 where  $L_s$  is the simulated sound pressure level in a 1/3 octave band and  $L_m$  is the  
20 measured sound pressure level in the same band. The summation is taken over the  
21 interested frequencies. It should be noted that a set of scaling constant  $a_i$  is only valid  
22 for a specific tire and a range of pavement texture depth. The model should be  
23 recalibrated if tire characteristics or pavement properties vary significantly. After  
24 proper calibration is performed, the model is then validated against noise  
25 measurements on other pavement sections with various surface textures.

26 The CPX measurements conducted by Schwanen et al. (24) are used for this  
27 purpose. A continental slick tire (195/65R15) was tested in the noise measurements on  
28 a closed road paved with various surface layer types. Only dense-graded surfaces with  
29 very low acoustic absorption coefficients (i.e. below 0.1 in most of the measured  
30 frequency range) are involved in this section. Information of these examined surfaces  
31 is presented in Table 1. CPX method specified in ISO 11819-2 standard (25) was  
32 performed to measure the near field noise level. A vehicle with steady speed towed a  
33 trailer mounted with test tire, around which microphones were setup at specific close  
34 proximity positions. No enclosure was used around the tire since there was no other  
35 traffic at the test site (24). The distance between the test tire and the towing vehicle  
36 was more than 5 m to prevent the interference from towing vehicle noise. The A-  
37 weighted sound pressure level (both overall level and 1/3-octave bands) is measured  
38 along with vehicle speed.

39 An FE tire model is built based on the geometry and the properties of test tire  
40 and its vibration characteristics are simulated using the developed analysis framework.  
41 Pavement surface texture was measured using laser profilometer on each section and  
42 the resulting texture level spectra were made available in the project report by  
43 Schwanen et al. (25). Force excitations on tire tread at the contact patch is generated  
44 using the texture spectra obtained from the experiments. These force excitations  
45 induce tire vibrations which then provide the boundary conditions of BEM acoustic  
46 model. Because there was no enclosure in the experiments performed by Schwanen et



al. (24), wind on the site can create errors in the low-frequency domain. As such, measured noise with frequency below 300 Hz are considered to be erroneous and are therefore removed from the database. The upper bound of interested frequency range is set to be 2500 Hz as Cesbron et al. (7) had shown in their earlier works that high frequency noise are likely to be generated from air pumping and frictional effect than from excitation due to pavement textures.

**TABLE 1 Specification and properties of pavement surfaces used in model calibration and validation (24)**

Section No.	Pavement type	Surface layer thickness (mm)	Mean profile depth (mm)	British pendulum number
S01	ISO surface	30	0.39	89.0
S02	Thin asphalt layer 2/4	25	0.45	90.5
S03	Thin asphalt layer 2/6	25	0.56	91.0
S04	Thin asphalt layer 2/6	25	0.75	90.0
S05	Thin asphalt layer 4/8	25	0.93	89.5
S19	SMA 0/6	20	0.52	80.5
S20	SMA 0/8	25	0.89	82.0
S21	SMA 0/11	30	1.11	85.5
S22	SMA 0/16	40	1.38	85.5
S23	DAC 0/16	40	0.46	87.5
S40	Surface dressing 5/8	n.a.	3.16	n.a.
S41	Surface dressing 11/16	n.a.	5.99	n.a.

Note: n.a. means that the data is not available.

Calibration was performed separately for high-texture pavements (MPD above 0.5 mm) and low-texture pavements (MPD below 0.5 mm). Noise measurement at 70 km/h speed on a Stone Mastic Asphalt (SMA) surface (S20, MPD = 0.89) was used to calibrate high-texture model and that on a dense asphalt concrete (DAC) surface (S23, MPD = 0.46) was used for low-texture model. With this effort, two sets of calibrated parameters are made available for pavements with high texture depths and low texture depths respectively. Validation of the high-texture and low-texture models were performed on the asphalt sections and the results are shown in Table 1. The simulated and measured 1/3-octave spectra are shown in Figure 3, and the simulated overall noise levels and measured results are compared in Figure 4 and Table 2 respectively. It can be seen from the figures that with proper calibration, the developed model can adequately predict the overall noise levels as well as the noise spectra on dense-graded pavements. The errors of overall noise levels are found to be within  $\pm 2$  dB(A) (with the exception of one case) and the predicted 1/3-octave spectra can basically describe the measured spectrum shapes.

1  
2 **TABLE 2 Model validation results of overall noise levels**  
3

Section No.	Measured Sound Pressure Level (SPL) [dB(A)]	Simulated Sound Pressure Level (SPL) [dB(A)]	Error [dB(A)]
S01	86.2	85.5	-0.7
S02	83.4	82.2	-1.2
S03	84.0	82.7	-1.3
S04	84.7	86.2	1.5
S05	87.9	88.1	0.2
S19	86.1	85.4	-0.7
S20	89.8	88.6	-1.2
S21	91.6	90.7	-0.9
S22	92.8	92.2	-0.6
S23	88.4	87.3	-1.1
S40	97.4	93.4	-4.0
S41	100.3	100.0	-0.3

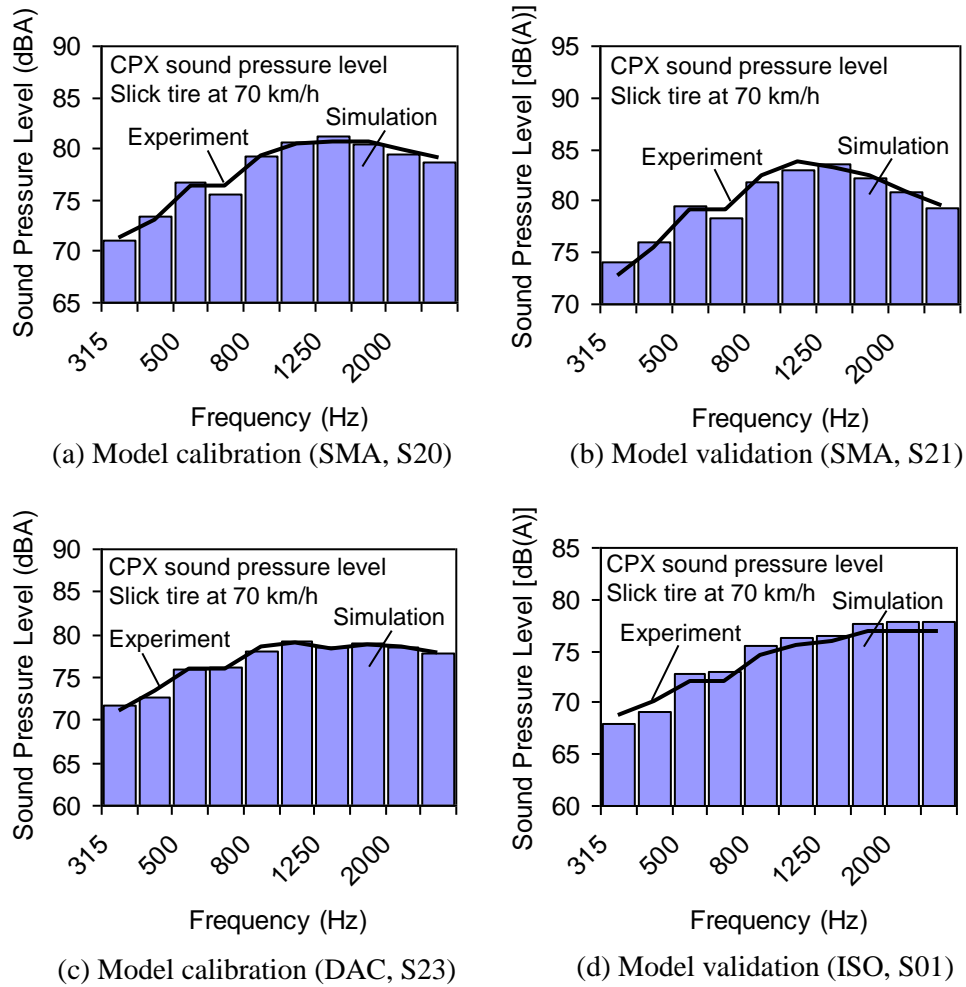
4  
5  
6 **EFFECT OF PAVEMENT TEXTURE ON TIRE-ROAD NOISE**  
7

8 Five types of dense-graded asphalt pavements tested in the experiments by Schwanen  
9 et al. (24), namely ISO standard surface, thin layered asphalt (TLA), stone mastic  
10 asphalt (SMA), dense asphalt concrete (DAC) and surface dressing (SD), are  
11 considered in this paper in evaluating the effect of pavement surface texture on tire-  
12 road noise. Texture profiles of the test sections were measured by high-resolution  
13 laser profilometer on the wheel paths. Texture spectrum for each test section was  
14 computed from the measured texture profile. The transformation of texture from space  
15 domain to frequency domain was performed using Fourier transformation and the  
16 conversion of texture amplitude from height (mm) to power level (dB) is defined by:

$$17 \quad L_{tx,f} = 20 \log(a_f / a_{ref}) \quad (10)$$

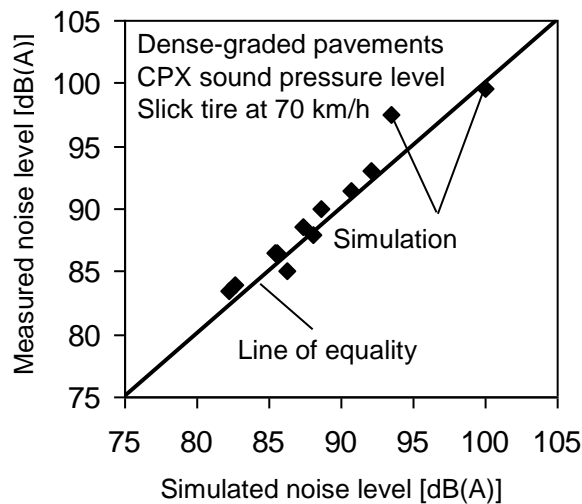
18 where  $L_{tx,\lambda}$  is the texture level for the 1/3-octave band with median frequency  $f$ ,  $a_f$  is  
19 the root mean square amplitude for surface profile height variations in the frequency  
20 band, and  $a_{ref}$  is a reference texture amplitude ( $10^{-6}$  m).

21 Mean profile depth (MPD), estimated texture depth (ETD) and root mean  
22 square (RMS) were also derived from the measured profiles. Acoustic absorption  
23 measurements showed that most of the dense-graded surfaces were acoustically hard  
24 with absorption coefficient less than 0.1 over the measured frequency range.  
25 Therefore, the perfect reflection assumption holds for all the dense-graded surfaces  
26 analyzed in this study.  
27



1  
2  
3

**FIGURE 3 Illustration of simulated and measured 1/3-octave spectra (refer to Table 1 for surface type).**

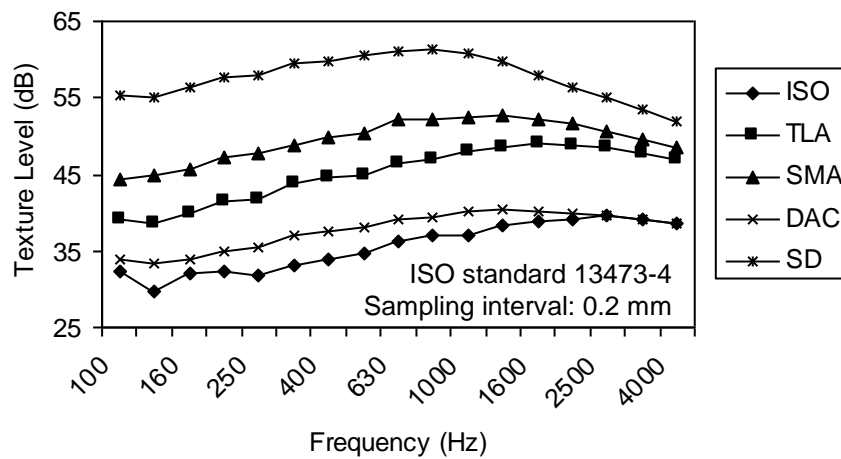


4  
5  
6  
7  
8

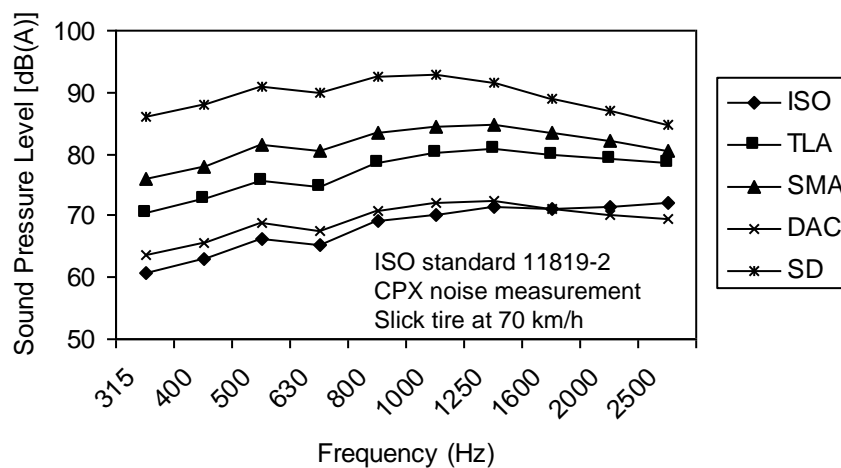
**FIGURE 4 Comparison between simulated and measured overall noise levels.**

**Effect of Pavement Surface Type on Tire Vibration Noise**

Numerical simulations using the developed framework were performed at a traveling speed of 70 km/h on the test sections and the effect of pavement type, texture depth and aggregate size on tire/road noise are analyzed. Figure 5(a) shows the texture spectra for each pavement type presented in Table 2. It is observed from the figure that surface dressing has a highest texture amplitude which ranges from 100 to 4000 Hz (corresponding to a wavelength range from 5 to 200 mm at a 70 km/h vehicle speed). This may be attributed to the large aggregate size (11/16) used in this surface type. The SMA surface with a 16 mm nominal maximum aggregate size has the second highest texture level among the five pavement types. Dense asphalt concrete surface with the same 16 mm aggregate size has a much lower texture level compared to that of SMA. The ISO surface possesses the lowest texture level, which is expected since the ISO-10844 surface is considered to be a standard smooth pavement surface.



(a) Texture spectra



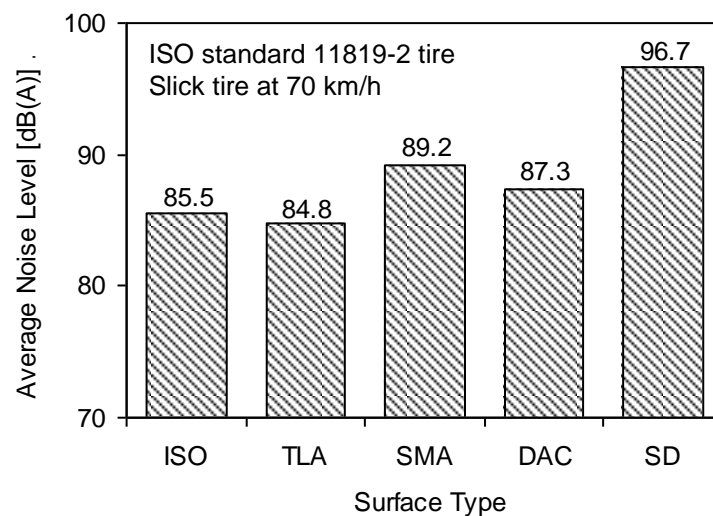
(b) Simulated sound spectra

**FIGURE 5 Effect of pavement surface type on tire/road noise emission.**

The simulated 1/3-octave band spectra of CPX noise level for the five pavement types are shown in Figure 5(b). It can be seen from the figure that surface dressing (SD) produces the highest noise level over the 300 to 2500 Hz frequency

1 range while the ISO surface is the quietest. The differences in sound pressure levels  
 2 on various pavements are larger at low frequencies and smaller at high frequencies.  
 3 Compared to the texture spectra shown in Figure 5(a), it was found that the surface  
 4 type with a higher texture level usually generates higher noise when the identical tire  
 5 travels on various pavements at the same speed.

6 The overall noise level can be determined from the 1/3-octave band spectrum  
 7 and the results are shown in Figure 6. It was found that surface dressing has the  
 8 highest overall noise level, followed by stone mastic asphalt (SMA) and dense-graded  
 9 asphalt (DAC) surfaces. Thin layered asphalt (TLA) and the ISO surfaces are  
 10 considered quiet. The difference in overall noise levels can be as high as 12 dB(A)  
 11 among five pavement surface types considered in the paper.  
 12

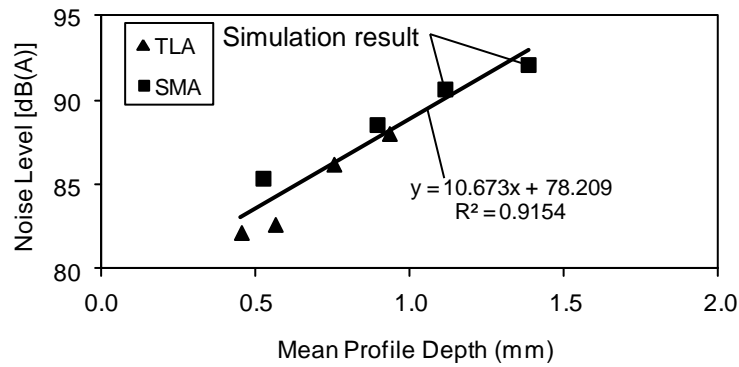


13  
 14 **FIGURE 6 Average noise level for different pavement surface types.**

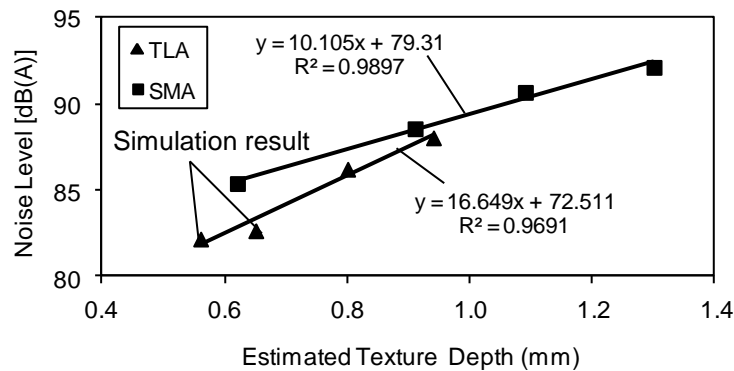
### 15 16 **Effect of Texture Depth on Tire-Road Noise**

17  
 18 It can be seen from the earlier analyses that different pavement surface textures (and  
 19 their texture spectra) can result in significantly different noise levels. As such, it may  
 20 be worthwhile to test if a plausible relationship between texture depth and noise level  
 21 can be obtained. There are many texture indices used in practice such as the mean  
 22 profile depth (MPD), estimated texture depth (ETD) and the root mean square (RMS)  
 23 depth which could be used to test if they are well correlated to tire-road noise.

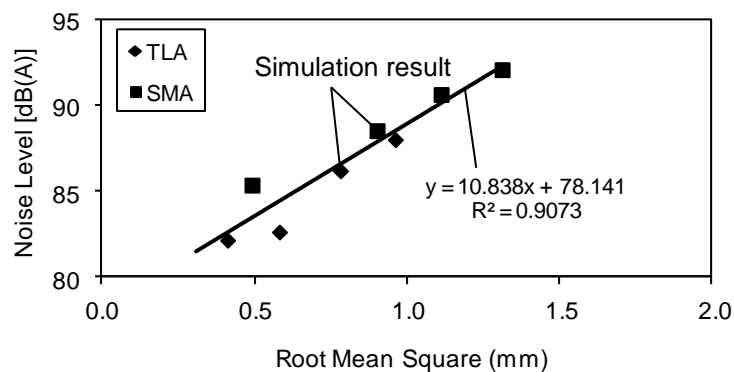
24 Mean profile depth (MPD), estimated texture depth (ETD) and root mean  
 25 square (RMS) for thin layered asphalt (TLA) (Sections S02 to S05 in Table 1) and  
 26 stone mastic asphalt (SMA) (Sections S19 to S22 in Table 1) were studied to evaluate  
 27 if any meaningful relationship between these texture indices and noise can be  
 28 obtained. The developed regression relationships are shown in Figure 7. The  
 29 relationship between mean profile depth (MPD) and the overall noise level is shown  
 30 in Figure 7(a). It can be seen from the figure that tire-road noise increases when MPD  
 31 increases. The linear relationship from the figure suggests that noise level increases by  
 32 approximately 1.1 dB(A) for every 0.1 mm increment in MPD.



(a) Mean profile depth (MPD)



(b) Estimated texture depth (ETD)



(c) Root mean square (RMS)

**FIGURE 7 Relationship between noise level and texture indices.**

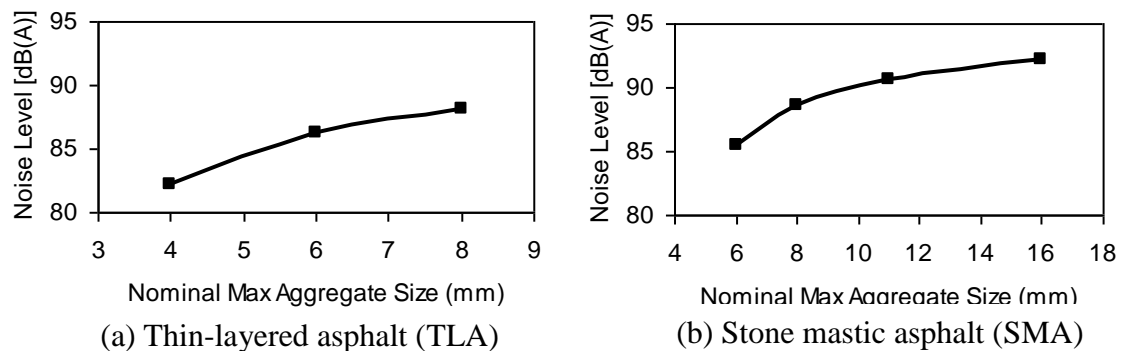
Figure 7(b) plots relationship between noise level and estimated texture depth (ETD). Even though ETD is linearly correlated to MPD (26), the relationship between ETD and texture depth is found to be non-linear. In fact, the relationship is found to be pavement surface type dependent, as shown in Figure 7(b). It can be seen from the figure that in general, noise level increases as ETD increases. Noise level increases by about 1.6 dB(A) on thin layered asphalt (TLA) surfaces and by about 1.0 dB(A) on SMA surfaces for every 0.1 mm increase in ETD.

Figure 7(c) shows the relationship between root mean square (RMS) and the overall noise level. It is observed that there is a 1.1 dB(A) increase in the overall noise level for every 0.1 mm increase in RMS value.

1  
2  
3  
4  
5  
6  
7  
8  
9  
10  
11  
12  
13  
14

## 1 Influence of Aggregate Size on Tire-Road Noise

2  
3 The difference in surface texture for the surface types listed in Table 1 could be a  
4 result of the different aggregate sizes used in the mix design and the effect of  
5 aggregate size on tire-road noise is studied. The nominal maximum aggregate size  
6 (NMAS) is an important index in the gradation design, representing the overall  
7 aggregate size level and the NMAS values for TLA (Sections S02 to S05 in Table 1)  
8 and stone mastic asphalt (SMA) (Sections S19 to S22 in Table 1) were obtained from  
9 Schwanen et al. (24). The simulated noise levels on these surfaces are plotted against  
10 NMAS values, as shown in Figure 8. It can be seen that tire-road noise increases in a  
11 nonlinear manner when larger aggregates are used.



12  
13 **FIGURE 8 Relationship between noise level and NMAS.**

## 14 CONCLUSION

15  
16  
17 Finite element method and boundary element method are integrated into a numerical  
18 simulation model analyzing the effect of pavement surface texture on the noise  
19 generated from tire-pavement interaction. Four steps are performed sequentially in  
20 this model framework where tire rolling conditions, tire natural frequencies and mode  
21 shapes, tire wall vibration characteristics and noise level emanating from tire vibration  
22 were computed. Calibration and validation of the model were performed and the  
23 model was applied on five pavements surface types (in twelve test sections) to  
24 simulate the noise generated on these pavements. The CFX noise level on each test  
25 section is predicted and is found to fit well to the measured experimental noise levels.  
26 The effects of pavement surface texture on tire-road noise is studied and the below  
27 major findings are found:

- 28 • Pavement type has a significant influence on tire/road noise level. Surface  
29 dressing generates the highest noise level and thin layered asphalt surfaces has  
30 the lowest average overall noise level.
- 31 • Overall noise level increases when pavement texture depth increases.
- 32 • For a given pavement type, noise level increases when the nominal maximum  
33 aggregate size used in the mix design increases.

34 While the model is considered to be adequate for most pavement engineering  
35 applications, additional future work would have to be made to include other noise  
36 generation mechanisms (such as the air-pumping effect and the horn effect).

37  
38

1 **REFERENCES**

- 2
- 3 1. den Boer, L. C., and A. Schrotten. *Traffic Noise Reduction in Europe: Health*
- 4 *Effects, Social Costs and Technical and Policy Options to Reduce Road and*
- 5 *Rail Traffic Noise*. Delft, the Netherland, 2007.
- 6 2. Sandberg, U., and J. A. Ejsmont. *Tyre/Road Noise Reference Book*.
- 7 INFORMEX, Kisa, Sweden, 2002.
- 8 3. Eisenblaetter, J., S. J. Walsh, and V. V. Krylov. Air-Related Mechanisms of
- 9 Noise Generation by Solid Rubber Tyres with Cavities. *Applied Acoustics*, Vol.
- 10 71, No. 9, 2010, pp. 854-860.
- 11 4. Kim, B. S., G. J. Kim, and T. K. Lee. The Identification of Sound Generating
- 12 Mechanisms of Tyres. *Applied Acoustics*, Vol. 68, No. 1, 2007, pp. 114-133.
- 13 5. Koizumi, T., N. Tsujiuchi, R. Tamaki, and T. Iwagase. An Analysis of
- 14 Radiated Noise from Rolling Tire Vibration. *JSAE Review*, Vol. 24, No. 4,
- 15 2003, pp. 465-469.
- 16 6. Kindt, P., D. Berckmans, F. De Coninck, P. Sas, and W. Desmet.
- 17 Experimental Analysis of the Structure-Borne Tyre/Road Noise Due to Road
- 18 Discontinuities. *Mechanical Systems and Signal Processing*, Vol. 23, No. 8,
- 19 2009, pp. 2557-2574.
- 20 7. Cesbron, J., F. Anfosso-Lédée, D. Duhamel, H. P. Yin, and D. Le Houédec.
- 21 Experimental Study of Tyre/Road Contact Forces in Rolling Conditions for
- 22 Noise Prediction. *Journal of Sound and Vibration*, Vol. 320, No. 1-2, 2009, pp.
- 23 125-144.
- 24 8. Kim, B. S. Sound Radiation due to Tire Tread Vibration. *JSME International*
- 25 *Journal. Series C, Mechanical Systems, Machine Elements and Manufacturing*,
- 26 Vol. 46, No. 2, 2003, pp. 675-682.
- 27 9. Fujikawa, T., H. Koike, Y. Oshino, and H. Tachibana. Definition of Road
- 28 Roughness Parameters for Tire Vibration Noise Control. *Applied Acoustics*,
- 29 Vol. 66, No. 5, 2005, pp. 501-512.
- 30 10. O'Boy, D. J., and A. P. Dowling. Tyre/Road Interaction Noise - Numerical
- 31 Noise Prediction of a Patterned Tyre on a Rough Road Surface. *Journal of*
- 32 *Sound and Vibration*, Vol. 323, No. 1-2, 2009, pp. 270-291.
- 33 11. Brinkmeier, M., U. Nackenhorst, S. Petersen, and O. von Estorff. A Finite
- 34 Element Approach for the Simulation of Tire Rolling Noise. *Journal of Sound*
- 35 *and Vibration*, Vol. 309, No. 1, 2008, pp. 20-39.
- 36 12. Kropp, W., P. Sabiniarz, H. Brick, and T. Beckenbauer. On the Sound
- 37 Radiation of a Rolling Tyre. *Journal of Sound and Vibration*, Vol. 331, No. 8,
- 38 2012, pp. 1789-1805.
- 39 13. Tuononen, A. J. Laser Triangulation to Measure the Carcass Deflections of a
- 40 Rolling Tire. *Measurement Science and Technology*, Vol. 22, No. 12, 2011, pp.
- 41 125-304.
- 42 14. Faria, L. O., J. M. Bass, J. T. Oden, and E. B. Becher. A Three-Dimensional
- 43 Rolling Contact Model for a Reinforced Rubber Tire. *Tire Science Technology*,
- 44 Vol. 17, No. 3, 1989, pp. 217-233.
- 45 15. Nackenhorst, U. The ALE-Formulation of Bodies in Rolling Contact.
- 46 *Computer Methods in Applied Mechanics and Engineering*, Vol. 193, No. 39,
- 47 2004, pp. 4299-4322.



- 1 16. Chang, Y. B., T. Y. Yang, and W. Soedel. Dynamic Analysis of a Radial Tire  
2 by Finite Elements and Modal Expansion. *Journal of Sound and Vibration*,  
3 Vol. 96, No. 1, 1984, pp. 1-11.
- 4 17. Reddy, J. N. *Mechanics of laminated composite plates: theory and analysis*,  
5 CRC Press, Boca Raton, 1997.
- 6 18. Ong, G. P., and T. F. Fwa. Wet-Pavement Hydroplaning Risk and Skid  
7 Resistance: Modeling. *Journal of Transportation Engineering*, Vol. 133, No.  
8 10, 2007, pp. 590-598.
- 9 19. Sabiniarz, P., and W. Kropp. A Waveguide Finite Element Aided Analysis of  
10 the Wave Field on a Stationary Tyre, not in Contact with the Ground. *Journal*  
11 *of Sound and Vibration*, Vol. 329, No. 15, 2010, pp. 3041-3064.
- 12 20. Lecomte, C., W. R. Graham, and M. Dale. A Shell Model for Tyre Belt  
13 Vibrations. *Journal of Sound and Vibration*, Vol. 329, No. 10, 2010, pp. 1717-  
14 1742.
- 15 21. Brinkmeier, M., and U. Nackenhorst. An Approach for Large-Scale  
16 Gyroscopic Eigenvalue Problems with Application to High-Frequency  
17 Response of Rolling Tires. *Computational Mechanics*, Vol. 41, No. 4, 2008,  
18 pp. 503-515.
- 19 22. Bathe, K. J. *Finite Element Procedures*, Prentice-Hall, Englewood Cliffs, New  
20 Jersey, 1996.
- 21 23. Rustighi, E., S. J. Elliott, S. Finnveden, K. Gulyás, T. Mócsai, and M. Danti.  
22 Linear Stochastic Evaluation of Tyre Vibration due to Tyre/Road Excitation.  
23 *Journal of Sound and Vibration*, Vol. 310, No. 4-5, 2008, pp. 1112-1127.
- 24 24. Schwanen, W., H. M. Leeuwen, A. A. A. Peeters, G. J. Blokland, H. F.  
25 Reinink, and W. Kropp. *Acoustic Optimization Tool RE3: Measurement Data*  
26 *Kloosterzande Test Track*. Delft, The Netherlands, 2007.
- 27 25. ISO. *Acoustics - Method for Measuring the Influence of Road Surfaces on*  
28 *Traffic Noise - Part 2: Close-Proximity Method (Draft)*. ISO/DIS 11819-2,  
29 International Organization for Standardization, Geneva, Switzerland, 2003.
- 30 26. ASTM. *Standard Test Method for Measuring Pavement Macrotexture Depth*  
31 *Using a Volumetric Technique*. American Society for Testing and Material,  
32 E965, West Conshohochen, Pennsylvania, 2006.